NUCL SCI TECH (2019) 30:140
https://doi.org/10.1007/s41365-019-0666-3

Research on the effect of the heavy nuclei amount on the temperature reactivity coefficient in a small modular molten salt reactor

Meng-Lu Tan[1,2] · Gui-Feng Zhu[1] · Yang Zou[1] · Xiao-Han Yu[1] · Ye Dai[1]

Received: 27 December 2018 / Revised: 8 April 2019 / Accepted: 14 May 2019 / Published online: 13 August 2019

Abstract Small modular thorium-based graphite-moderated molten salt reactors (smTMSRs), which combine the advantages of small modular reactors and molten salt reactors, are regarded as a wise development path to speed deployment time. In a smTMSR, low enriched uranium and thorium fuels are used in once-through mode, which makes a marked difference in their neutronic properties compared with the case when a conventional molten salt breeder reactor is used. This study investigated the temperature reactivity coefficient (TRC) in a smTMSR, which is mainly affected by the molten salt volume fraction (VF) and the heavy nuclei concentration in the fuel salt (HN). The four-factor formula method and the reaction rate method were used to indicate the reasons for the TRC change, including the fuel density effect, the fuel Doppler effect, and the graphite thermal scattering effect. The results indicate that only the fuel density has a positive effect on the TRC in the undermoderated region. Thermal scattering from both salt and graphite has a significant negative influence on the TRC in the overmoderated region. The maximal effective multiplication factor, which shows the highest fuel utilization, is located at 10% VF and 12 mol% HN and is still located in the negative TRC region. In addition, on increasing the heavy nuclei amount from 2 mol% HN to 12 mol% HN (VF = 10%), the total TRC undergoes an obvious change from − 11 to − 3 pcm/K, which implies that the change in the HN caused by the fuel feed online should be small to avoid potential trouble in the reactivity control scheme.

Keywords Molten salt reactor · Temperature reactivity coefficient · Heavy nuclei amount

1 Introduction

Change in the temperature of a nuclear reactor leads to change in the reactivity of the system, which is described in terms of the temperature reactivity coefficient (TRC) [1]. The TRC of a reactor must be negative to guarantee its self-control ability and thus plays a crucial role in reactor safety and operation. Molten salt reactors (MSRs) [2, 3] have special TRCs due to not only their high temperature materials, but also to their liquid nuclear fuel. In an MSR, the total reactivity feedback of temperature can be split into effects due to the graphite and those due to the fuel salt. The latter can be further split into the density effect and the Doppler effect.

At present, research into the TRC of MSRs is mostly based on ^{233}U–^{232}Th fuel in conventional molten salt breeder reactors (MSBRs) [4]. Many studies have shown that the TRC of the MSBR can be positive when the molten salt fraction increases, due to the positive graphite temperature reactivity coefficient (GTRC) [5–10]. One of the

This work is supported by the Chinese TMSR Strategic Pioneer Science and Technology Project (No. XDA02010000) and the Frontier Science Key Program of Chinese Academy of Sciences (No. QYZDY-SSW-JSC016).

✉ Gui-Feng Zhu
zhuguifeng@sinap.ac.cn

✉ Xiao-Han Yu
yuxiaohan@sinap.ac.cn

[1] Shanghai Institute of Applied Physics, Chinese Academy of Sciences, Shanghai 201800, China

[2] University of Chinese Academy of Sciences, Beijing 100049, China

positive contributions always comes from the graphite neutron scattering effect, which increases the thermal fission rate of ^{233}U when the temperature of graphite increases. Another positive contribution may come from the density effect of the salt in the undermoderated region. Therefore, many design optimizations of MSBRs have been performed to obtain a negative total TRC.

Recently, MSRs using low enriched uranium (LEU) with a once-through fuel cycle have aroused great interest around the world. During operation, LEU is added to the online reactor to compensate for the reactivity loss, and no chemical reprocessing is carried out. This kind of fuel cycle is derived from the denatured molten salt reactor (DMSR) [11], whose purpose is to minimize nuclear proliferation risk, and is currently implemented by ThorCon [12] and IMSR [13] for the rapid deployment of MSRs due to fuel availability and less technical challenges. Also, the LEU fuel cycle is adopted in the small modular thorium-based molten salt reactor (smTMSR), as the second stage of the thorium-based molten salt reactor (TMSR) nuclear energy system project launched by the Chinese Academy of Sciences (CAS) [9, 14, 15].

Two differences can be found in the LEU fuel cycle when compared with the fuel cycle in conventional MSBRs. One is that the fuel is ^{235}U–^{238}U or ^{235}U–^{238}U–^{232}Th instead of ^{233}U–^{232}Th; these different fission cross sections will bring about different Doppler effects and thermal scattering effects, especially in terms of the GTRC. Another is that the amount of heavy nuclei will escalate during the burnup life, which will contribute to a significant change in the neutron spectrum as well as the reaction rates of fuel, graphite, and other materials, leading to the change in the TRC [16, 17].

The TRCs in the LEU fuel cycle were calculated for some designs of MSR [8, 9, 15, 16, 18] to show their inherent safety, while less systematical research and the mechanism of the effect on the TRC have been carried out. In this paper, the fuel density coefficient, the fuel Doppler coefficient, and the GTRC of the smTMSR with different heavy nuclei amounts were analyzed. The four-factor formula method and reaction rate analysis were also employed to explain the changes in the TRC in the current study. Section 2 introduces the model of the smTMSR, and Sect. 3 introduces the research methods. Section 4 presents the results and analysis. The conclusion is given in Sect. 5.

2 Calculation model

The smTMSR is a 400-MWth thermal reactor based on modular technology. It can be applied in coastal areas such as the seaside, islands, and offshore platforms, and it can also be used in inland, mountainous, and mining areas.

A preliminary nuclear design of the smTMSR [19] is shown in Fig. 1 and Table 1. The core consists of hexagonal prism graphite blocks and the molten salt channels. Large graphite blocks are adopted to enhance the space self-shielding effect of ^{238}U. 30-cm-width graphite reflectors are added to reduce fast neutron irradiation of the Hastelloy reactor vessel. The core diameter is set as 4.4 m to improve the fuel utilization and lower the power density to extend the graphite irradiation life.

Changes in the heavy nuclei amount are mainly reflected in the mole concentration of heavy nuclei fuel in the molten salt (HN) and the volume fraction of molten salt in the active core (VF). In order to extensively investigate the effect of the heavy nuclei amount on the TRC, we varied the HN from 2 to 12 mol% (2, 4, 6, 8, 10, and 12 mol%) and the VF from 5 to 25% (5, 10, 15, 20, and 25%) at the beginning of the lifetime, which meant that a total of 25 different cores were calculated. The TRC was calculated from difference of 100 K (from 900 to 1000 K). The number of particles used in MCNP5 [20] was 500,000, and the number of total active cycles was 350. The statistical standard deviation of k_{eff} reached 0.00005. The ENDF/B-VII library was used in this calculation.

The ratios of fuel composition are mole ratios.

3 Four-factor formula method

One of the TRC analysis methods [22–24] used was the four-factor formula method. In this method,

$$k_\infty = f\eta p\varepsilon, \tag{1}$$

where k_∞ is the infinite multiplication factor, f is the thermal utilization factor, η is the thermal fission factor, p is the resonance escape probability, and ε is the fast fission factor.

The formula for each factor is: [25–27]

$$\varepsilon = \frac{\nu\sum_{f,1}^{f}\phi_1 + \nu\sum_{f,2}^{f}\phi_2}{\nu\sum_{f,2}^{f}\phi_2}, \tag{2}$$

$$p = \frac{\sum_{a,2}\phi_2}{\sum_{a,1}\phi_1 + \sum_{a,2}\phi_2}, \tag{3}$$

$$\eta = \frac{\nu\sum_{f,2}^{f}\phi_2}{\sum_{a,2}^{f}\phi_2}, \tag{4}$$

$$f = \frac{\sum_{a,2}^{f}\phi_2}{\sum_{a,2}\phi_2}, \tag{5}$$

where ν is the average fission neutrons produced for each fission, $\sum_{f,1}^{f}\phi_1$ is the fuel fast fission rate, $\sum_{f,2}^{f}\phi_2$ is the fuel thermal fission rate, $\sum_{a,2}\phi_2$ is the thermal absorption

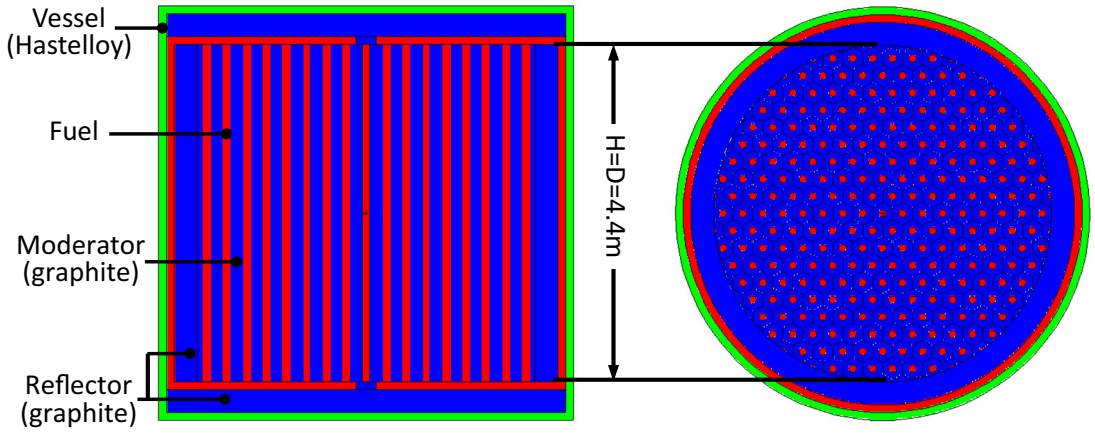

Fig. 1 (Color figure online) Longitudinal and transverse section of the smTMSR core

Table 1 Main parameters of the smTMSR core

Parameter	Value
Power (MWth)	400
Inlet/outlet temperature (°C)	600/700
Hexagonal graphite component pitch (cm)	26
Active region height/diameter (m)	4.4/4.4
Graphite reflector thickness (m)	0.3
Hastelloy vessel thickness (cm)	2
Fuel salt composition	$LiF:BeF_2$ = 73.83:18.99 $^{235}UF_4$:$^{238}UF_4$:ThF_4 = 0.17:0.68:6.33
^{7}Li enrichment (mol%)	99.995
900 K, fuel salt density (g/cm^3) [21] (HN = 2/4/6/8/10 mol%)	2.195/2.439/2.665/2.873/3.068
1000 K, fuel salt density (g/cm^3) (HN = 2/4/6/8/10 mol%)	2.156/2.397/2.619/2.825/3.017

rate, $\sum_{a,1}\phi_1$ is the fast absorption rate, and $\sum_{a,2}^{f}\phi_2$ is the fuel thermal absorption rate. The thermal energy group ranges from 0 to 0.625 eV, and the fast energy group ranges from 0.625 to 20 MeV.

According to the definition of the effective multiplication factor,

$$k_{\text{eff}} = f\eta p\varepsilon\Lambda, \tag{6}$$

where Λ is the non-leakage probability. In this study, Λ is the ratio of the core active area absorption rate to the total absorption rate.

The reaction rate of fission or absorption can be obtained using MCNP. Therefore, we can determine the values of f, η, p, ε and Λ.

The reactivity change per unit temperature change is the TRC, which can be expressed as:

$$\alpha_{\text{T}} = \frac{\partial\rho}{\partial T} = \frac{1}{k_{\text{eff}}}\frac{\partial k_{\text{eff}}}{\partial T} - \frac{k_{\text{eff}}-1}{k_{\text{eff}}^2}\frac{\partial k_{\text{eff}}}{\partial T}. \tag{7}$$

The reactivity changes for the individual factors are defined as: [28]

$$\alpha_{\text{T}}^{f} = \frac{\varepsilon p\eta\Lambda\Delta f}{\Delta T k_{\text{eff}}^2}, \alpha_{\text{T}}^{\eta} = \frac{\varepsilon pf\Lambda\Delta\eta}{\Delta T k_{\text{eff}}^2}, \alpha_{\text{T}}^{p} = \frac{\varepsilon pf\Lambda\Delta p}{\Delta T k_{\text{eff}}^2}, \alpha_{\text{T}}^{\varepsilon} = \frac{p\eta f\Lambda\Delta\varepsilon}{\Delta T k_{\text{eff}}^2}, \alpha_{\text{T}}^{\Lambda} = \frac{\varepsilon p\eta f\Delta\Lambda}{\Delta T k_{\text{eff}}^2} \tag{8}$$

Through combining Eqs. (6), (7), and (8), the sum is obtained as:

$$\alpha_{\text{T}} = \alpha_{\text{T}}^{f} + \alpha_{\text{T}}^{\eta} + \alpha_{\text{T}}^{p} + \alpha_{\text{T}}^{\varepsilon} + \alpha_{\text{T}}^{\Lambda}. \tag{9}$$

According to Eq. (9), the TRC can be approximately decomposed into five parts. In this way, the contribution of each factor to the TRC can be studied, and the main factors influencing the TRC can be obtained.

The TRC can be decomposed into the fuel TRC (FTRC) and the GTRC [6]. Based on the density change in the molten salt, the FTRC is divided into the TRC caused by the density effect (the fuel density coefficient) and the TRC resulting from the Doppler effect (the fuel Doppler coefficient). The GTRC, the fuel density coefficient, and the fuel Doppler coefficient can be calculated by the definition of the TRC. Therefore, the total TRC of the smTMSR can be expressed as:

$$\left(\frac{\mathrm{d}\rho}{\mathrm{d}T}\right)_{\text{total}} = \left(\frac{\mathrm{d}\rho}{\mathrm{d}T}\right)_{\text{fueldensity}} + \left(\frac{\mathrm{d}\rho}{\mathrm{d}T}\right)_{\text{doppler}} + \left(\frac{\mathrm{d}\rho}{\mathrm{d}T}\right)_{\text{graphite}}. \quad (10)$$

The fuel density reactivity coefficient is the change in the value of the core reactivity when the density of molten salt is changed via a one-unit rise in temperature and other conditions remain the same (including the temperature of the molten salt). For 2/4/6/8/10 mol% HN, the density of the molten salt changes from 2.195/2.439/2.665/2.873/3.068 to 2.156/2.397/2.619/2.825/3.017 g/cm^3 when the temperature is changed from 900 to 1000 K. The fuel Doppler coefficient and the GTRC are the changes in the values of the core reactivity per unit change in the molten salt and graphite, respectively, with all other conditions remaining the same.

Each part of the total TRC can be analyzed with Eq. (9) and is discussed separately below.

Based on the smTMSR model, the reliability of the four-factor method can be verified through comparing the TRCs calculated by Eqs. (9) and (7). The differences are shown in Table 2.

The statistical errors in the TRC calculated by the TRC definition and the four-factor formula method are ± 0.12 pcm/K and ± 0.31 pcm/K, respectively. According to Table 2, the differences are within the scope of the statistical error, and the calculation results were basically identical, proving that the four-factor method in the current work is reliable.

4 Results and discussion

4.1 Effective multiplication factor

Figure 2 shows the change in k_{eff} in the 25 different cases mentioned above, with the HN range 2–12 mol% and the VF range 5–25%. It can be seen that k_{eff} increases first and then decreases with increase in the VF. The gradient of k_{eff} as the heavy nuclei amount is decreased is significantly

Table 2 Difference in the total TRC calculated by the four-factor formula method and the TRC definition (pcm/K)

HN (mol%)	VF (%)				
	5	10	15	20	25
2	0.23	− 0.33	0.01	− 0.08	− 0.11
4	0.12	− 0.17	− 0.02	− 0.12	− 0.06
6	− 0.10	− 0.14	− 0.04	0.08	− 0.23
8	− 0.03	− 0.07	− 0.01	− 0.08	0.04
10	0.03	− 0.14	− 0.17	− 0.21	− 0.29

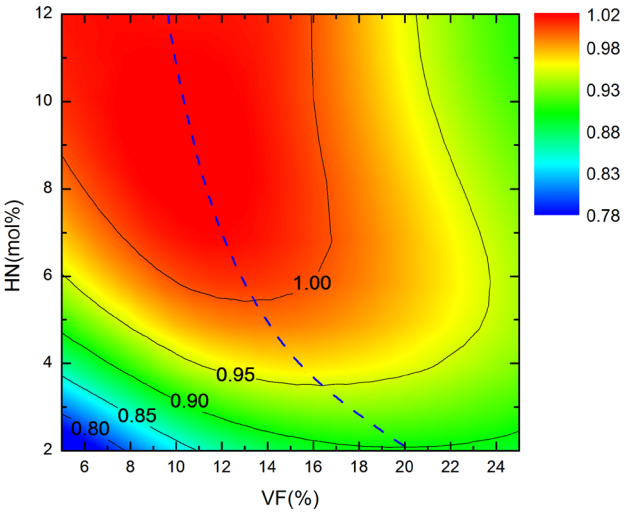

Fig. 2 (Color figure online) K_{eff} for different VFs and HNs. The dashed line represents the critical points of the overmoderated and the undermoderated region

larger. The maximal k_{eff}, which shows the highest fuel utilization, is located at 10% VF and 12 mol% HN. The dashed line connects the turning points of the contour lines in the direction of the VF. It indicates that k_{eff} increases as VF increases on the left side of the dashed line, and that k_{eff} decreases as VF decreases on the right side of the dashed line. Thus, the dashed line in Fig. 2 represents the critical points of the overmoderated region and the undermoderated region. Compared with the general MSBR, the critical points tend to occur at smaller VF [9]. Different kinds of driver fuel will lead to different locations of the critical points between the undermoderated region and the overmoderated region. For example, the fuel composition of the TMSR, which is a thorium-based MSBR [9], is 71.7 LiF + 16 BeF_2 + 12.3 (ThF_4 + $^{233}UF_4$), different from that of the smTMSR. The critical point is located at the point where the VF is about 17% and the HN is 12.3 mol% in the TMSR [9], although the VF of the smTMSR is near 10% with 12 mol% HN. The reason for the different critical points may be that the fission cross section of ^{235}U is larger than that of ^{233}U.

4.2 Fuel density coefficient

The fuel density coefficient is positively correlated with the heavy nuclei amount (VF and HN), as shown in Fig. 3. The absolute value of the negative coefficient decreases with increasing the heavy nuclei amount and then changes from negative to positive. The critical point curve of the fuel density temperature coefficient is almost the same as the critical point curve of the overmoderated region and the undermoderated region, as shown in Fig. 2. This is because the effect of the decrease in the fuel salt on the reactivity is

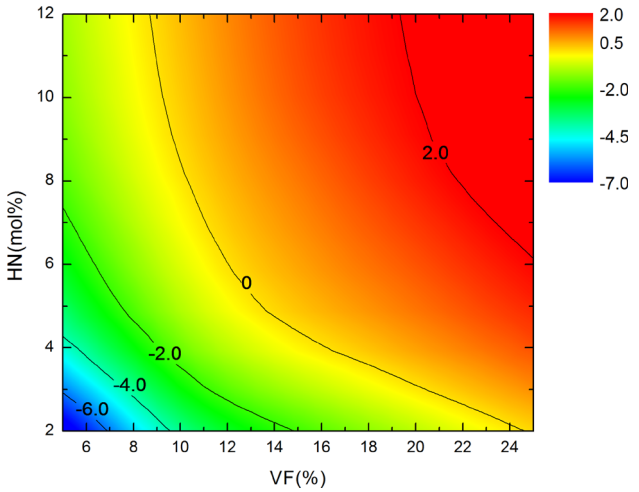

Fig. 3 (Color figure online) Fuel density coefficient for different VFs and HNs. The unit of the TRC in the figure and in all the other contour plots below is pcm/K

consistent with the VF decrease. As analyzed in Sect. 4.1, this implies that the VF of the smTMSR should be smaller than that of the TMSR in order to obtain a negative density effect.

The fuel density coefficient was further analyzed by the four-factor method, as presented in Fig. 4. The resonance escape coefficient has a significantly positive effect on the TRC in the undermoderated region; however, the thermal utilization coefficient and neutron leakage have an obviously negative influence on the TRC in the overmoderated region. In Figs. 5 and 6, two conditions (VF = 5%, HN = 2 mol% and VF = 20%, HN = 12 mol%) were chosen. The former condition is in the overmoderated region, and the latter is in the undermoderated region.

As observed in Fig. 5, the resonance escape coefficient is mainly affected by ^{232}Th. Because of the decrease in the fuel salt density, the ratio of moderation to fuel will increase and the neutron spectrum will be softer (Fig. 6).

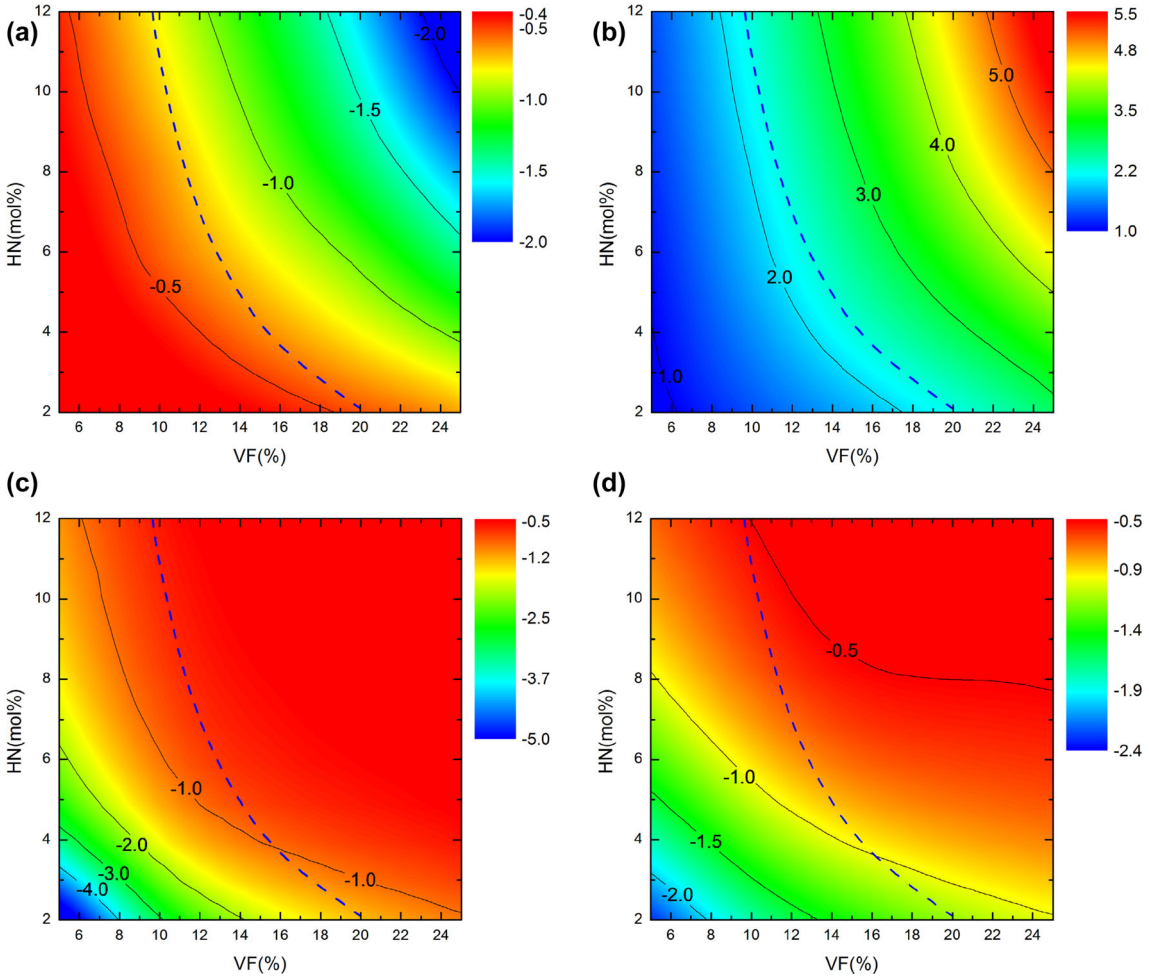

Fig. 4 (Color figure online) Factors that have a significant effect on the fuel density coefficient. **a** Fast fission coefficient α_T^{ε}, **b** resonance escape coefficient α_T^{p}, **c** thermal utilization coefficient α_T^{f}, and **d** non-leakage coefficient α_T^{A}

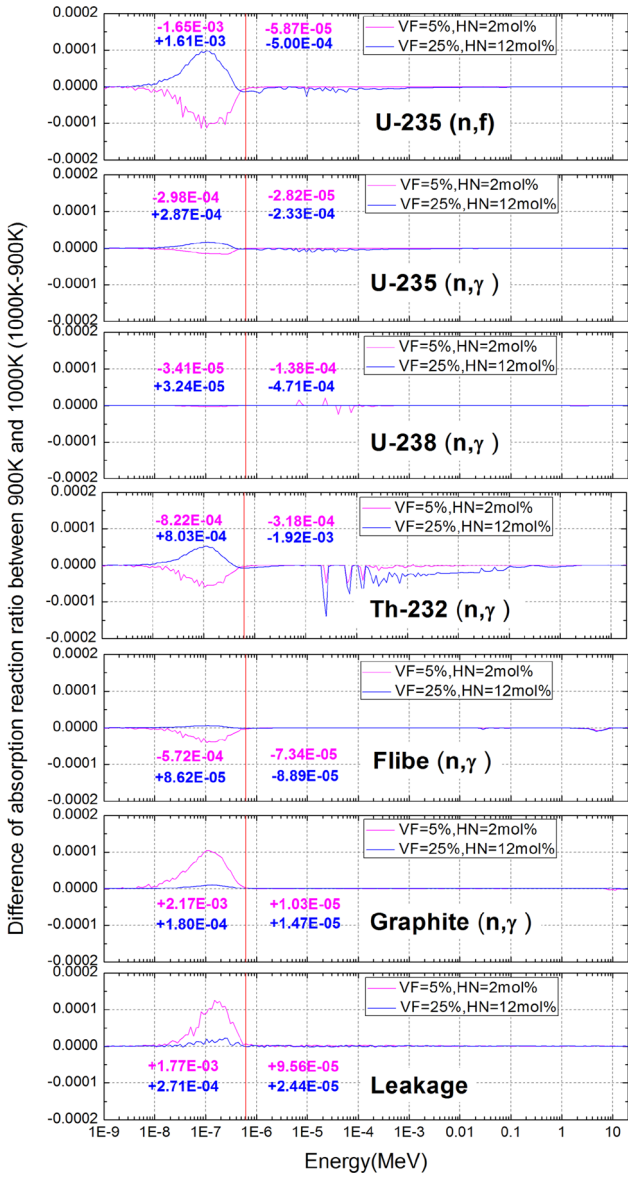

Fig. 5 (Color figure online) Change in the absorption reaction ratios when the fuel density is at temperatures from 900 to 1000 K. The red line is the boundary between the thermal region and the fast region. The numbers next to the lines are the integrals of the reaction rate in the thermal region and the fast region

More fast neutrons are moderated by graphite instead of absorbed by ^{232}Th in the resonance region. The resonance absorption of ^{232}Th causes an obvious decrease in the undermoderated region when the fuel salt density decreases, so that the resonance escape coefficient is positive and will be more obvious in the undermoderated region.

The thermal utilization coefficient is mainly caused by neutron absorption by the graphite, as shown in Fig. 5. When the fuel salt density decreases and the ratio of moderation to fuel increases, the neutron absorption by graphite increases, especially in the overmoderated region.

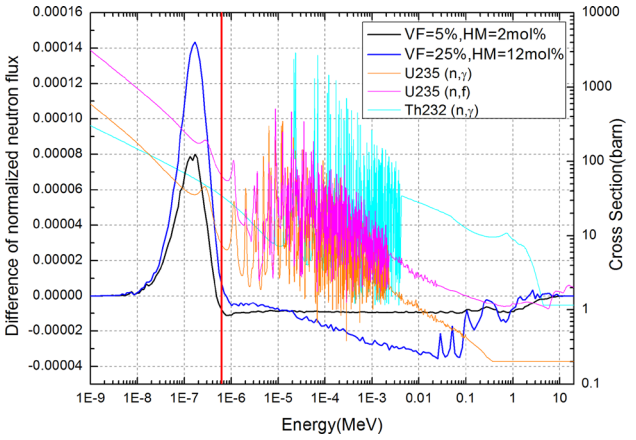

Fig. 6 (Color figure online) Microscopic cross sections and change in the neutron spectrum when the fuel density is at temperatures from 900 to 1000 K

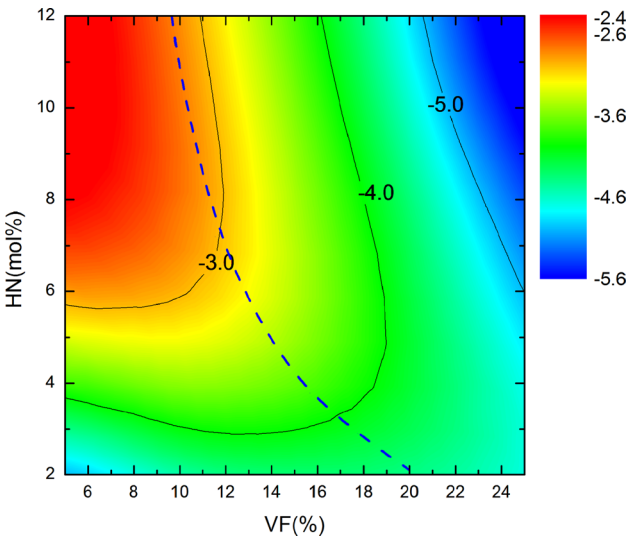

Fig. 7 (Color figure online) Fuel Doppler coefficients for different VFs and HNs

Thus, the thermal utilization coefficient is negative. In the undermoderated region, the thermal neutron absorption increases because the neutron resonance escape probability increases. However, as the increase in graphite absorption decreases, so does the value of the thermal utilization coefficient. Neutron leakage is similar to graphite absorption; therefore, the non-leakage coefficient is negative and the absolute value decreases with the increase in the heavy nuclei amount.

4.3 Fuel Doppler coefficient

Figure 7 presents the fuel Doppler coefficient for different VFs and HNs. The resonance escape coefficient has a significantly positive effect on the TRC in the undermoderated region; however, the thermal utilization

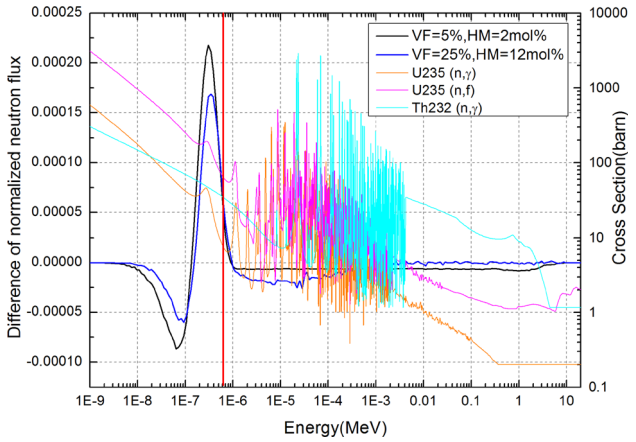

Fig. 8 (Color figure online) Microscopic cross sections and changes in the neutron spectrum with fuel temperatures from 900 to 1000 K

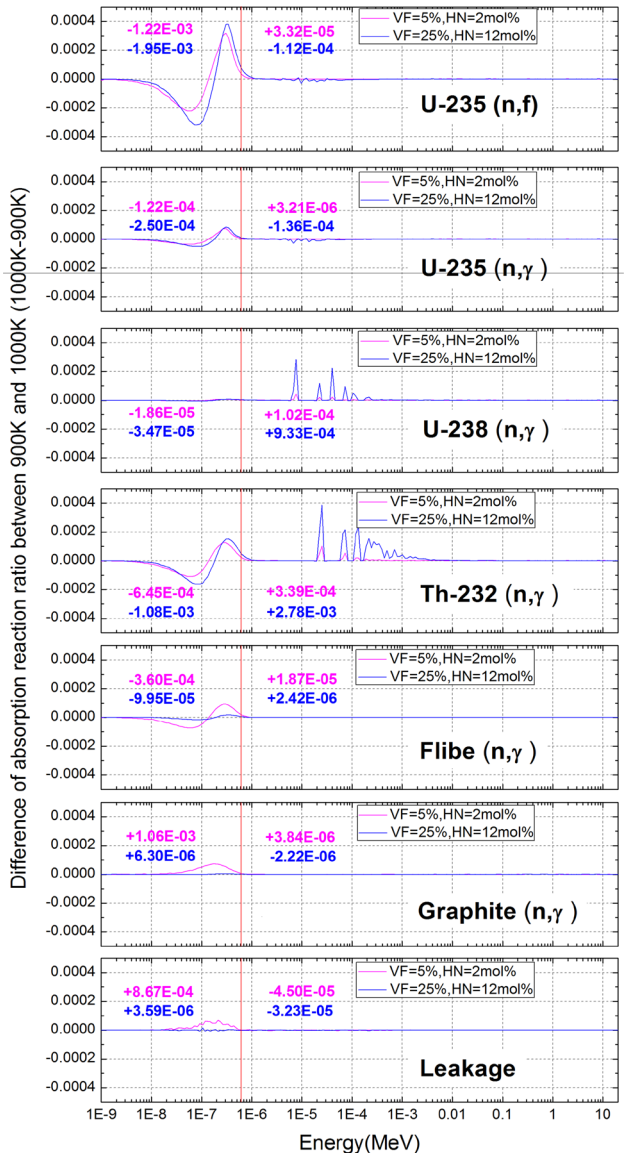

Fig. 9 Change in the absorption reaction ratios with fuel temperatures from 900 to 1000 K

coefficient and neutron leakage have a negative influence on the TRC in the overmoderated region. The Doppler effect [3, 29] will broaden the resonance peaks of heavy nuclei and reduce the energy self-shielding effect because of the rise in the temperature of the fuel salt, increasing the neutron resonance absorption. Usually, fertile fuels such as ^{238}U and ^{232}Th have higher resonance peaks than fission fuels like ^{235}U, as shown in Fig. 8. More neutrons are absorbed by ^{232}Th and ^{238}U than by ^{235}U (Fig. 9), especially in the undermoderated region. Therefore, the fuel Doppler coefficient caused by the resonance escape coefficient is always negative and is inversely proportional to the heavy nuclei amount, as shown in Fig. 10a.

The other main factors of the fuel Doppler coefficient come from the thermal utilization coefficient and non-leakage coefficient in the overmoderated region, as shown in Fig. 10b, c. It is noteworthy that the carrier fluoride salt is also a moderator. The Maxwell peak shifts to the high-energy region because the temperature increases (Fig. 8). The thermal scattering of the carrier salt increases, so the fission of ^{235}U decreases and the graphite absorption and leakage increase (Fig. 9). The fission cross section of ^{235}U decreases faster, which will make the decrease in the fission reaction more serious. The increase in the graphite absorption and the decrease in ^{235}U fission lead to a negative thermal utilization coefficient. The increase in leakage results in a negative non-leakage coefficient. These effects are more obvious in the overmoderated region, and therefore, the thermal utilization coefficient and the non-leakage coefficient are more negative (Fig. 8).

4.4 Fuel temperature reactivity coefficient

The sum of the fuel density coefficient and the fuel Doppler coefficient is the FTRC, as shown in Fig. 11. The FTRC is positively correlated with the heavy nuclei amount (VF and HN). The absolute value of the negative coefficient decreases with the increase in the heavy nuclei amount. Compared with TMSR [9], the FTRC in the smTMSR with 12 mol% HN and the same VF showed little difference, as shown in Table 3. In the low HN region, the fuel density effect and the Doppler effect both lead to a deeply negative TRC. This will lead to a significant change in the TRC during the operation of the smTMSR when the HN is continuously refueled from 6 mol% (if the VF = 10% and the initial k_{eff} is close to 1) to 12 mol%. This will not happen in the TMSR because the heavy nuclei will be conservative and always be kept at around 12% mol HN [9].

4.5 Graphite temperature reactivity coefficient

Figure 12 presents the graphite reactivity coefficient for different VFs and HNs. The graphite temperature coefficient is always negative and becomes more negative with lower heavy nuclei amount, which is different from the Th–U cycle in TMSR [9]. In the TMSR, the graphite temperature reactivity coefficient is positive and decreases with increasing VF.

The thermal utilization coefficient plays a significant positive role in the overmoderated region; however, the neutron leakage has an obvious negative influence on the undermoderated region. Similar to the salt effect analyzed in subsection 4.3, the graphite thermal scattering is enhanced and the Maxwell peak shifts to the higher energy region; hence, the neutron spectrum becomes harder (Fig. 13). Since the fission cross section of ^{235}U decreases faster than the absorption cross section of ^{232}Th, the hardening of the energy spectrum leads to more decrease in the ^{235}U fission. As a result, the neutron leakage increases, which has a negative effect on the TRC, as shown in Fig. 14b. In the TMSR, the rate of decrease in the fission cross section of ^{233}U is slower, so the thermal scattering of graphite has a positive contribution. However, the graphite absorption probability decreases, as shown in Fig. 15, which has a positive effect on the thermal utilization coefficient, as shown in Fig. 14a. The neutron leakage is more obvious than the decrease in the neutron absorption by graphite. As a result, the GTRC is negative. With higher heavy nuclei amounts, the neutron leakage will decrease, and the decrease in the graphite absorption will become smaller, so the absolute value of the GTRC will decrease (Fig. 13).

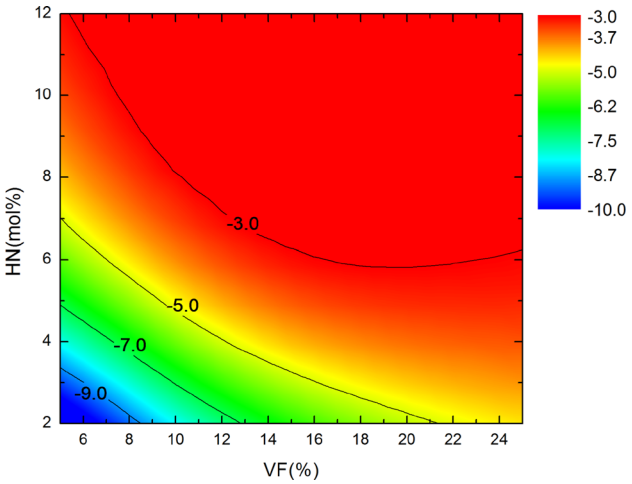

Fig. 11 (Color figure online) Fuel temperature reactivity coefficient for different VFs and HNs

Table 3 Fuel temperature reactivity coefficient of the TMSR and smTMSR with 12 mol% HN (pcm/K)

Reactor	VF (%)			
	5	10	15	20
TMSR	− 3.2	− 2.5	− 2	− 2.3
smTMSR	− 3.1	− 2.5	− 2.3	− 2.5

4.6 Total temperature reactivity coefficient

Figure 16 shows the total TRC of the smTMSR for different VFs and HNs. The total temperature coefficients are negative (− 15 to − 3 pcm/K) in the range 5–25% VF and 2–12 mol% HN. In Fig. 16, the main factors affecting the temperature coefficient in the undermoderated and overmoderated region are added. Only the fuel density

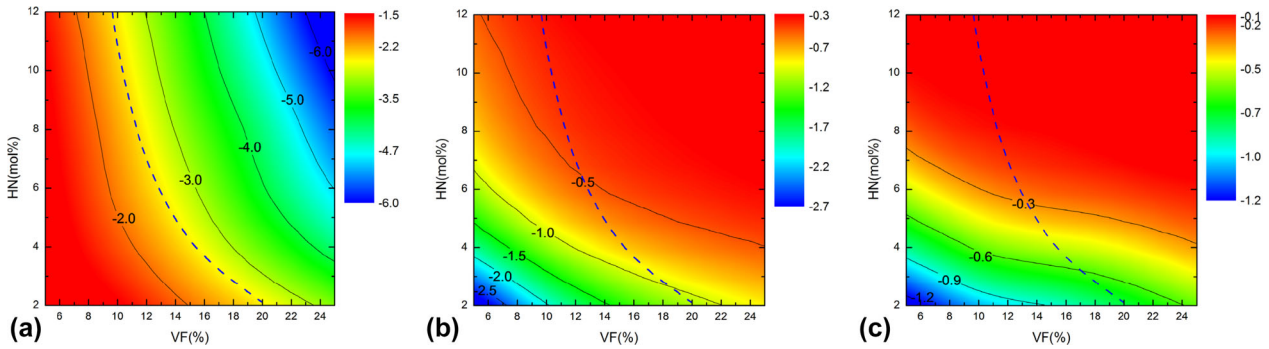

Fig. 10 (Color figure online) Factors that have a significant effect on the fuel Doppler coefficient. **a** Resonance escape coefficient α_T^p, **b** thermal utilization coefficient α_T^f, **c** non-leakage coefficient α_T^A

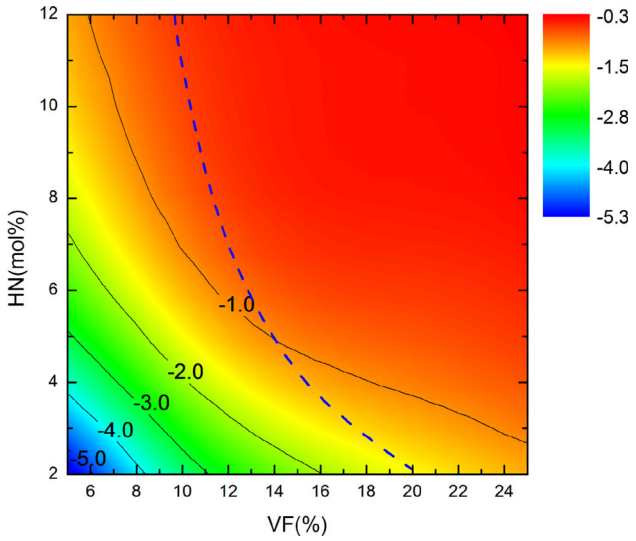

Fig. 12 (Color figure online) GTRC for different VFs and HNs

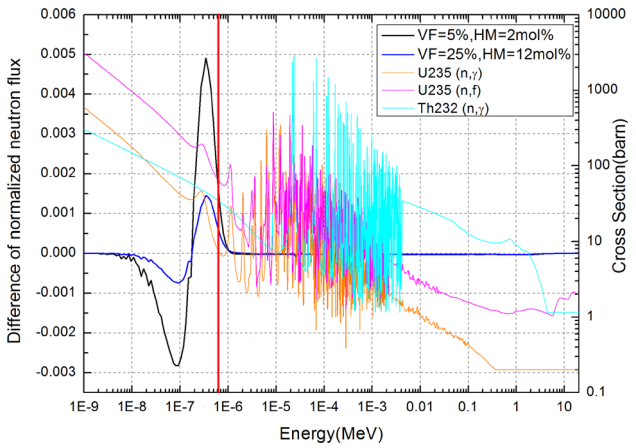

Fig. 13 (Color figure online) Microscopic cross sections and changes in the neutron spectrum for graphite temperatures from 900 to 1000 K

effect has a positive effect on the TRC in the undermoderated region. All other factors make a negative contribution. The fuel Doppler coefficient mainly contributes in the undermoderated region. In addition, the thermal scattering from both the salt and graphite has a significant influence on the overmoderated region.

5 Conclusion

The effect of the VF and HN on the TRC of the smTMSR has been analyzed in this paper. The four-factor formula method and reaction rate method were used to determine the reasons for the changes in the TRC, including the fuel density effect, the fuel Doppler effect, and the carrier salt and graphite thermal scattering. Because the driver fuel and fuel cycle mode in the smTMSR are different from those in the TMSR, some new findings can be summarized as follows:

1. The fuel density effect in the undermoderated region is positive and is mainly caused by the resonance escape of fertile fuel, whereas in the overmoderated region, the fuel density effect is negative because the graphite absorption and the neutron leakage play a leading role. The VF in the smTMSR should be smaller than that in the TMSR in order to obtain a negative density effect, possibly because the cross section of ^{235}U is larger than that of ^{233}U.
2. The thermal scattering effects of both salt and graphite are obviously negative in the overmoderated region. The thermal scattering effect of graphite is the main reason for the negative GTRC, whereas the contribution of this effect is positive in TMSR. This is because

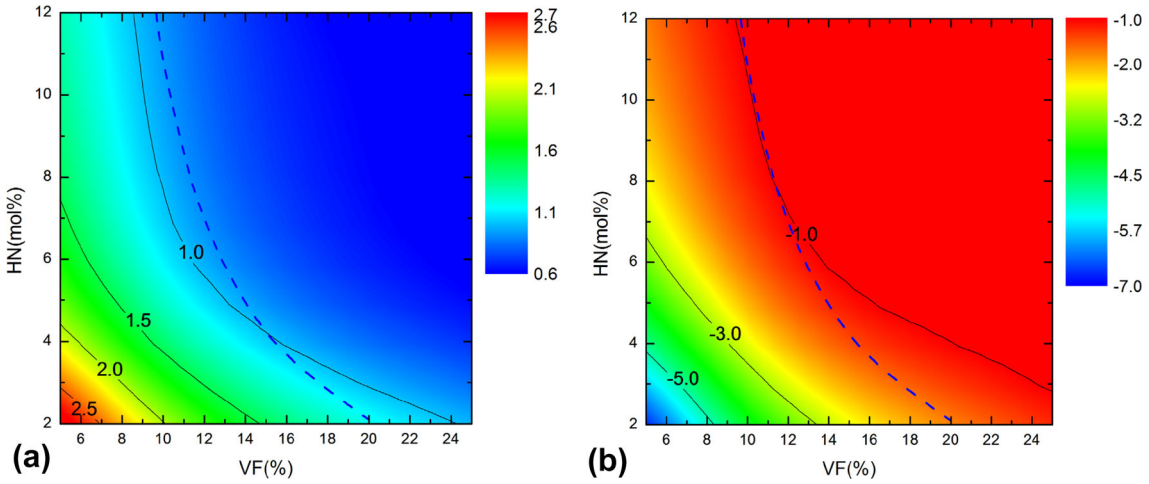

Fig. 14 (Color figure online) Factors that have a significant effect on the GTRC. **a** Thermal utilization coefficient α_T^f, **b** non-leakage coefficient α_T^A

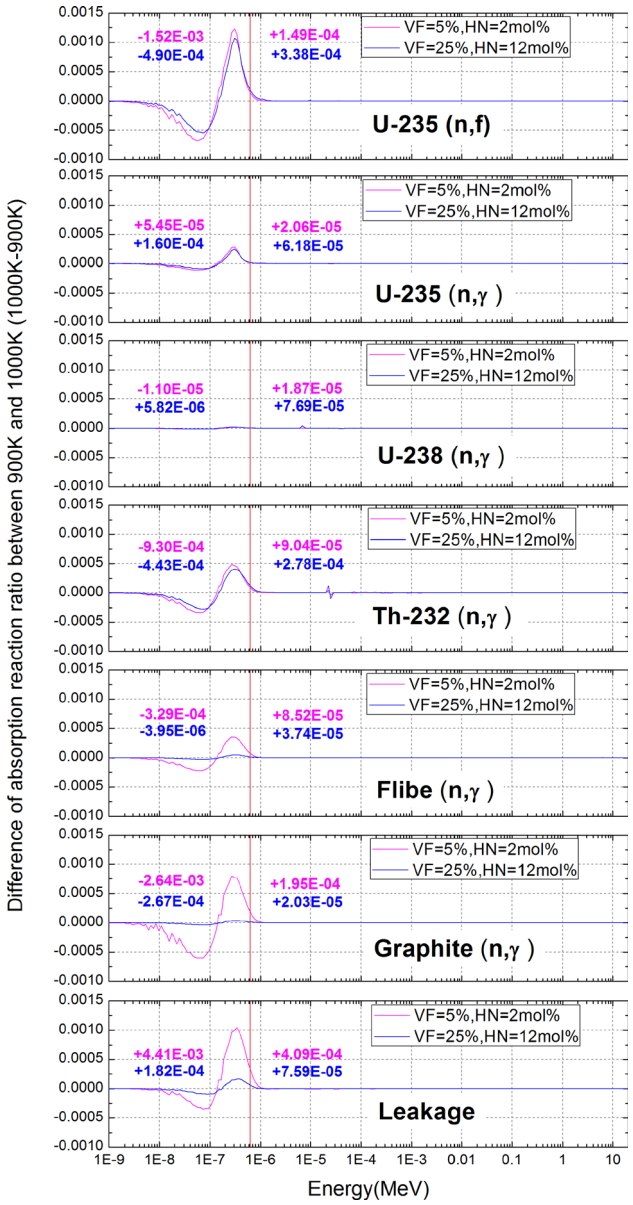

Fig. 15 Changes in the absorption reaction ratios for graphite temperatures from 900 to 1000 K

the fission cross section of ^{235}U falls faster in the thermal region than that of ^{233}U.

3. The total TRCs are negative (− 15 to − 3 pcm/K) for 5–25% VF and 2–12 mol% HN. The inherent safety in the beginning can be guaranteed. The maximal k_{eff} is located at 10% VF and 12 mol% HN, and the TRC is still negative. In addition, with increasing the heavy nuclei amount from 2 mol% HN to 12 mol% HN (VF = 10%) in the beginning, the total TRC will show an obvious change from − 11 to − 3 pcm/K, which implies that the change of HN caused by fuel feed online should be small to lower potential problems in the reactivity control scheme. As the burnup increases, the fission products and ^{233}U will increase, which could both have a positive effect on the TRC; this should be further analyzed and studied.

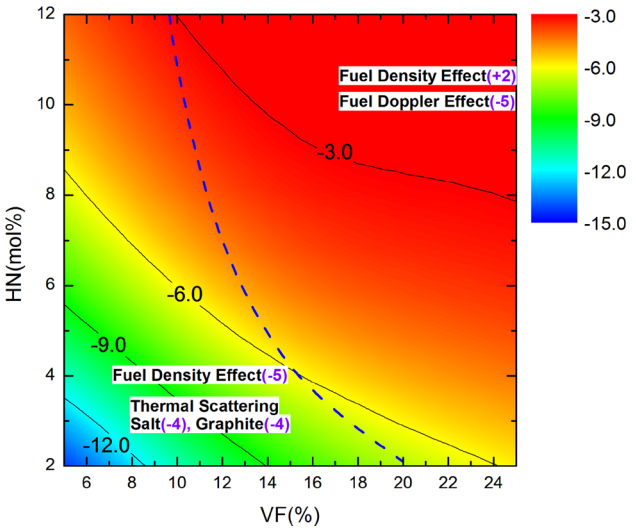

Fig. 16 (Color figure online) Total TRC for different VFs and HNs

References

1. J. Serp, M. Allibert, O. Beneš et al., The molten salt reactor (MSR) in generation IV: overview and perspectives. Prog. Nucl. Energy **77**, 308–319 (2014). https://doi.org/10.1016/j.pnucene.2014.02.014
2. J. Krepel, B. Hombourger, V. Bykov et al., Molten salt reactor with simplified fuel recycling and delayed carrier salt cleaning, *Paper Presented at the 22th International Conference on Nuclear Engineering ICONE'22*, Prague, July 2014
3. H. Omar, K. Khattab, N. Ghazi, Feedback reactivity coefficients for the Syrian MNSR research reactor. Prog. Nucl. Energy **54**(1), 162–166 (2012). https://doi.org/10.1016/j.pnucene.2011.07.001
4. J.E. Kelly, Generation IV international forum: a decade of progress through international cooperation. Prog. Nucl. Energy **77**, 240–246 (2014). https://doi.org/10.1016/j.pnucene.2014.02.010
5. C.L. Brun, L. Mathieu, D. Heuer et al., Impact of the MSBR concept technology on long-lived radio-toxicity and proliferation resistance, *Paper Presented at Technical Meeting on Fissile Material Management Strategies for Sustainable Nuclear Energy*, Vienna, Sept 2005
6. L. Mathieu, D. Heuer, R. Brissot et al., The thorium molten salt reactor: moving on from the MSBR. Prog. Nucl. Energy **48**(7), 664–679 (2006). https://doi.org/10.1016/j.pnucene.2006.07.005
7. L. Mathieu, D. Heuer, E. Merle et al., Possible configurations for the thorium molten salt reactor and advantages of the fast non-moderated version. Nucl. Sci. Eng. **161**, 78–89 (2009). https://doi.org/10.13182/NSE07-49
8. K. Nagy, Dynamics and fuel cycle analysis of a graphite-moderated molten salt nuclear reactor, Delft University of Technology, 2012. https://doi.org/10.4233/uuid:b4d5089d-c2de-446b-94cf-c563dd73e8f1
9. C.Y. Zou, X.Z. Cai, D.Z. Jiang et al., Optimization of temperature coefficient and breeding ratio for a graphite-moderated

molten salt reactor. Nucl. Eng. Des. **281**, 114–120 (2015). https://doi.org/10.1016/j.nucengdes.2014.11.022
10. D. Heuer, E. Merle-Lucotte, M. Allibert et al., Towards the thorium fuel cycle with molten salt fast reactors. Ann. Nucl. Energy **64**, 421–429 (2014). https://doi.org/10.1016/j.anucene.2013.08.002
11. J.R. Engel, H.F. Bauman, J.F. Dearing et al., Conceptual design characteristics of a denatured molten-salt reactor with once-through fueling. Oak Ridge National Lab. ORNL/TM-7207 (1980). https://doi.org/10.2172/5352526
12. http://thorconpower.com/. Accessed 20 Jul 2018
13. L. Samalova, O. Chvala, G.I. Maldonado, Comparative economic analysis of the integral molten salt reactor and an advanced PWR using the G4-ECONS methodology. Ann. Nucl. Energy **99**, 258–265 (2017). https://doi.org/10.1016/j.anucene.2016.09.001
14. X.Z. Cai, Z.M. Dai, H.J. Xu. Thorium molten salt reactor nuclear energy system. Phys. **9**, 531–540 (2016)
15. G.C. Li, P. Cong, C.G. Yu et al., Optimization of Th–U fuel breeding based on a single-fluid double-zone thorium molten salt reactor. Prog. Nucl. Energy **108**, 144–151 (2018)
16. G.C. Li, Y. Zou, C.G. Yu et al., Influences of 7Li enrichment on Th–U fuel breeding for an improved molten salt fast reactor (IMSFR). Nucl. Sci. Tech. **28**, 97 (2017). https://doi.org/10.1007/s41365-017-0250-7
17. E. Merlelucotte, D.Heuer, M.Allibert et al. Optimization and simplification of the concept of non-moderated thorium molten salt reactor, *Paper Presented at International Conference on the Physics of Reactors "Nuclear Power: A Sustainable Resource"*, Casino-Kursaal Conference Center, Interlaken, 14–19 Sept 2008
18. B.R. Betzler, S. Robertson, E.E. Davidson et al., Assessment of the neutronic and fuel cycle performance of the transatomic power molten salt reactor design. Oak Ridge National Lab. ORNL/TM-2017/475 (2017). https://doi.org/10.2172/1410921
19. G.F. Zhu, Y. Zou, R. Yan, et al. Low enriched uranium and thorium fuel utilization under once-through and offline reprocessing scenarios in small modular molten salt reactor. Int. J. Energy Res. (2019). https://doi.org/10.1002/er.4676
20. X.-5 M.C. Team, MCNP—A general Monte Carlo N-particle transport code, Version 5. Los Alamos Nuclear Lab **2**, 71–80 (2005)
21. D.F. Williams, Assessment of candidate molten salt coolants for the Advanced High Temperature Reactor (AHTR). Oak Ridge National Lab. ORNL/TM-2006/12 (2006). https://doi.org/10.2172/885975
22. F. Ganda, E. Greenspan, Analysis of reactivity coefficients of hydride-fueled PWR cores. Nucl. Sci. Eng. **164**, 1–32 (2010). https://doi.org/10.13182/NSE08-64
23. U. Kannan, S. Ganesan, Analysis of coolant void reactivity of advanced heavy water reactor (AHWR) through isotopic reaction rates. Nucl. Sci. Eng. **167**, 105–121 (2011). https://doi.org/10.13182/NSE10-17
24. A. Sarkar, U. Kannan and P.D. Krishnani, Energywise contributions of Th, Pu & U isotopes to the reactivity feedbacks of (Th–LEU) fuelled AHWR. *Paper presented at the Thorium Energy Conference 2015 (ThEC15)*, Mumbai, 12–15 Oct 2015. https://doi.org/10.1007/978-981-13-2658-5_29
25. C.Y. Li, R.J. Sheu, J.J. Peir et al., Neutronic analyses of the HTTR core fueled with plutonium and minor actinides. *Paper presented at the 2013 21st International Conference on Nuclear Engineering*, 29 July–2 Aug, Chengdu, 2013. https://doi.org/10.1115/icone21-16507
26. C.W. Lau, C. Demazière, H. Nylén et al., Improvement of LWR thermal margins by introducing thorium. Prog. Nucl. Energy **61**, 48–56 (2012). https://doi.org/10.1016/j.pnucene.2012.07.004
27. X.X. Li, Y.W. Ma, C.G. Yu et al., Effects of fuel salt composition on fuel salt temperature coefficient (FSTC) for an under-moderated molten salt reactor (MSR). Nucl. Sci. Technol. **29**(8), 110 (2018). https://doi.org/10.1007/s41365-018-0458-1
28. J. Sun, Y. Zou, R. Yan et al., Analysis of the coolant reactivity coefficients of FHRs with 6Li contents of coolant. Nucl. Tech. **37**(9), 090605 (2014). https://doi.org/10.11889/j.0253-3219.2014.hjs.37.090605. **(in Chinese)**
29. Z. Jitka, T. Alberto, Analysis of the reactivity coefficients of the advanced high-temperature reactor for plutonium and uranium fuels. Ann. Nucl. Energy **35**(5), 904–916 (2008). https://doi.org/10.1016/j.anucene.2007.09.003